

## Synthesis and Characterization of Modified Multi-Walled Carbon Nanotubes Filled Thermoplastic Natural Rubber Composite

<sup>1</sup>Chita Ranjan Biswal, <sup>2</sup>Kampal Mishra and <sup>1</sup>P.L. Nayak

<sup>1</sup>P.L. Nayak Research Foundation and Synergy Institute of Technology, Bhubaneswar

<sup>2</sup>Department of Physics, SOA University, Odisha, India

**Abstract:** In the present research program, we have described the synthesis of acid doped TPNR nanocomposites were prepared by melt blending of PP, NR and LNR with MWCNTs in a ratio of 70 wt% PP, 20 wt% NR and 10wt% LNR as a compatibiliser and 1,3,5 and 7% via in situ polymerization. The structure of Maleic anhydride-grafted-polypropylene (MAPP) –TPNR (MWCNT) composites were characterized by X-ray, FTIR, Transmission Electron Microscopy (TEM) and mechanical, Thermal could be observed. The individual. The homogeneous dispersion of two types of the MWNTs throughout the TPNR matrix and strong interfacial adhesion between the MWCNTs and the matrix as confirmed by the TEM images are proposed to be responsible for the significant mechanical enhancement.

**Key words:** Multi-walled carbon nanotube • Thermal conductivities • Liquid natural rubber

### INTRODUCTION

The extraordinary properties of carbon nanotubes make them very promising and favorable as fillers for fabrication of a new class of polymeric heterostructures. Polymer matrices have been widely exploited as a medium for CNTs[1-6]. Research projects are focused on the development of CNT-based polymer materials that utilize the carbon nanotubes characteristics and properties. The grafting of polycationic electrolytes to defect sites of CNT has been studied [7, 8]. The free carboxylic acid functions on oxidized CNT were converted to acyl chlorides [9,10]. The activated tubes were mixed with poly-(propionylethyleneimine-co-ethyleneimine) and the polymer bound nanotubes were isolated upon amidation reaction. By microscopy studies, it was found that the polymer chains were attached mainly at the tips of the CNT. Using an alternative approach, direct heating of oxidized nanotubes in the polymer melt gave soluble functionalized material [6, 9].

Polypropylene (PP) is one of the most important plastics as it has an excellent balance of mechanical properties, melt flow, color stability, chemical residence and moisture barrier properties together with low cost. However, critical disadvantages for wider application

of this material are its low impact strength and non-polar and inert nature which result in difficulties in blending, coating and inking [11-14]. Functionalization of PP with polar molecules is the most attractive method to improve the properties of this material. By far, Maleic anhydride (MA) is the most important molecule in this context and MA modified PP has been prepared for commercial purposes and used to improve the polarity, compatibility and interaction of polypropylene with other materials. The grafting reaction normally is carried out by a radical mechanism1: Peroxide initiator provides radicals, some of which abstract hydrogen from the PP tertiary carbon to form PP macroradicals [16-17].

We wish to describe the synthesis and characterization of Maleic anhydride-grafted-polypropylene (MAPP) and TPNR nanocomposites were prepared by melt blending of PP, NR and LNR with MWCNTs in a ratio of 70 wt% PP, 20 wt% NR and 10wt% LNR as a compatibiliser and 1,3,5 and 7%. The polymer were characterized by a number of techniques including Fourier Transform Infrared Spectroscopy (FTIR), Transmission Electron Microscope (TEM) and X-ray diffraction (XRD), Tensile Strength, Impact strength and Thermal conductivity.

**Corresponding Author:** Dr. P.L. Nayak, R & D Director of Centre for Excellency Nanoscience and Technology, Synergy Institute of Technology, Odisha, India. Tel: +91-671-2441635.

## MATERIALS AND METHODS

Maleic anhydride, polypropylene were purchased from Aldrich. Multiwalled carbon nanotube (>90% purification) used in this work was purchased from Cheap Tubes (USA, 10–20 nm diameter) and Hindustan scientific Pvt. Other reagents like ammonium persulfate (APS), hydrochloric, sulfuric and nitric acid (Sigma Chemicals) were of analytical grade. Liquid natural rubber (LNR) was prepared by the photochemical degradation technique.

**Preparation of TPNR-Multi-Walled Carbon Nanotubes (MWCNTs) Composite:** Mixing was performed by an internal mixer (Haake Rheomix 600P). The mixing temperature was 180°C, with a rotor speed of 100 rpm and 13 min mixing time. The indirect technique (IDT) was used to prepare nanocomposites, this involved mixing the MWCNTs with LNR separately, before it was melt blended with PP and NR in the internal mixer. TPNR nanocomposites were prepared by melt blending of PP, NR and LNR with MWCNTs in a ratio of 70 wt% PP, 20 wt% NR and 10wt% LNR as a compatibiliser and 1,3,5 and 7% MWCNTs [8].

**Acid Treatment of MWCNTs:** Two types of MWCNTs were introduced to the TPNR which is untreated MWCNTs (MWCNTs 1) and treated MWCNTs (MWCNTs 2), MWCNTs 2 were treated by immersing neat MWCNTs in a mixture of nitric and sulfuric acid with a molar ratio of 1:3, respectively. In a typical experiment, 1g of raw MWCNTs was added to 40ml of the acid mixture. Then, the oxidation reaction was carried out in a two-necked, round-bottomed glass flask equipped with reflux condenser, magnetic stirrer and thermometer. The reaction was carried out for 3 hours at 140°C. After that, this mixture was washed with distilled water on a sintered glass filter until the pH value was around 7 and was dried in a vacuum oven at 70°C for 24hours [18-21].

### Characterizations

**X-Ray Diffraction (XRD) Measurement:** XRD measurements were carried out with a Rigaku Geiger Flex D/max\_RB X-ray diffractometer, CuK radiation, scanning at rate 2°/min.

**FTIR Spectroscopy:** FTIR spectra of the samples were recorded with a Nicolet 560 FTIR spectrometer in the range of 2000cm<sup>-1</sup>-400cm<sup>-1</sup> with an averaging of 32 scans at a resolution of 4 cm<sup>-1</sup>. The sample was prepared using the KBr pellet technique.

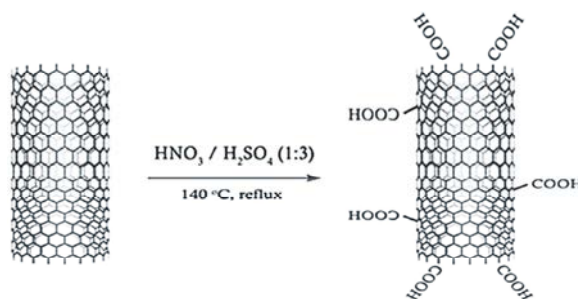


Fig. 1: Schematically modified of chemical functionalization of carbon nanotubes

**Transmission Electron Microscope (TEM) Measurement:** The dispersity of OMMT in the matrix was evaluated by TEM (Tecnai™ G2 20). Samples were prepared by frozen section procedure.

**Mechanical Properties:** The extrudates in 2.4 were pelletized and then molded into dumbbell-shaped tensile bars (GB1040---1992, 150 mm × 10 mm × 4 mm) and rectangular bars (ISO179---1999, 80mm X 10mm X 2mm). The measurements of the mechanical properties were carried at 25°C, humidity 65%. The tensile property was measured according to ASTM D638--2003, using an Instron 5500 Series Mechanical Tester. Impact strength measurement was carried out by a CEAST Resil impactor.

**Tensile Strength:** The tensile properties were tested using a Testometric universal testing machine model M350-10CT with 5 kN load cell according to ASTM 412 standard procedure using test specimens of 1 mm thickness and a crosshead speed 50 mm min<sup>-1</sup>. At least five samples were tested for each composition and the average value was reported.

**Impact Strength:** The impact test was carried out using a Ray Ran Pendulum Impact System according to ASTM D 256-90b. The velocity and weight of the hammer were 3.5m/s and 0.898kg, respectively.

**Thermal Conductivity:** The thermal conductivity was measured by a laser flash method. Disk-type samples (12.7 mm in diameter and 1mm in thickness) were set in an electric furnace Specific heat capacities were measured with a differential scanning calorimeter DSC. Thermal diffusivity ( $\lambda$ , Wm<sup>-1</sup> K<sup>-1</sup>) was calculated from thermal diffusivity ( $\alpha$ , m<sup>2</sup> s<sup>-1</sup>), density ( $\rho$ , g cm<sup>-3</sup>) and specific heat capacity ( $C_p$ , J g<sup>-1</sup> K<sup>-1</sup>) at each temperature.

$$\lambda = \alpha \cdot \rho \cdot C.$$

## RESULT AND DISCUSSION

**XRD Measurements:** Figure 2 demonstrates the XRD patterns of the composite with different content of Maleic anhydride-grafted-polypropylene (MAPP). It was seen that in the absence of MAPP only the  $\alpha$ -phase crystal phase of polypropylene was formed<sup>16</sup>. However, after the addition of maleic anhydride modified APP, a new peak at  $2\theta = 16.0^\circ$  and a slight increase of the peak at  $2\theta = 21.1^\circ$  relative to the peak at  $\sim 21.8^\circ$  are observed, attribute to the  $\beta$ -phase crystallization of polypropylene<sup>17</sup>. The introduction of MAPP thus causes the formation of hexagonal  $\beta$ -phase crystals, which are known to have greater mechanical absorption capacity than their  $\alpha$ -crystalline counterparts. Therefore, the presence of the  $\beta$ -phase crystalline in the composite contributes to the increase of the impact strength<sup>17, 18</sup>. No significant difference in the XRD pattern was observed between the composites containing different proportions of MAPP, however [22, 23].

**Fourier-Transform Infrared Spectroscopy:** MWCNTs were oxidized and purified by eliminating impurities such as amorphous carbons, graphite particles and metal catalysts [24]; the functional group of the surface of the CNTs are as shown in Figure 3. The generation of chemical functional groups on MWCNTs was confirmed using Fourier transform infrared spectroscopy (FT-IR) spectra which were recorded between  $400\text{ cm}^{-1}$  and  $4000\text{ cm}^{-1}$ . The FT-IR spectra of pure MWCNTs and the surface treated MWCNTs are shown in Figure 3a, b. The characteristic bands due to generated functional groups are observed in the spectrum of each chemically treated MWCNTs. In Figure 3a we could not see any band compared with the treated MWCNTs. The acid treated MWCNTs shows new peaks in comparison with

the FT-IR spectrum of the untreated MWCNTs, which lack the hydroxyl and carbonyl groups. The peaks around  $1581\text{ cm}^{-1}$  are assigned to the O–H band in C–OH and the peaks at  $673\text{ cm}^{-1}$  are assigned to COOH, as shown in Figure 3b. This demonstrates that hydroxyl and carbonyl groups have been introduced on the nanotube surface [25].

**Transmission Electron Microscopy (TEM):** TEM microphotographs of pure MWCNTs are shown in Figure 4 (A and B). The Figure 4 a presents unmodified MWCNTs and containing particles with diameters of 5-12 nm. The nanoparticles may be impurities from amorphous carbon and can be removed by acid treatment. According to the supplier, the unmodified MWCNT contains approximately 5% amorphous carbon. Figure 4 B displayed no nanoparticles in the acid-modified MWCNTs. The particles might have been removed during acid modification. This reveals that the acid-modified MWCNTs were straight and that some of them aggregated in bundles, which were dispersed well in the matrix. The length of the MWCNTs were reduced during acid modification, since the mixed acid corroded the MWCNTs. TEM microphotographs of the unmodified and acid-modified, curled and entangled MWCNTs demonstrate that the MWCNTs are straight [26].

Figure 4 C shows the good dispersion of 3wt% of UTMWCNTs inside TPNR and exhibits the better interfacial adhesion of UTMWCNTs and TPNR, Figure 4 D, 7wt% of UTMWCNTs, shows the poor dispersion and the large UTMWCNTs agglomerates of UTMWCNTs. This is because of the huge surface energy of MWCNTs, as well as, the weak interfacial interaction between UTMWCNTs and TPNR, which leads to inhomogeneous dispersion in the polymer matrix and negative effect on the properties of the resulting composites that causes a

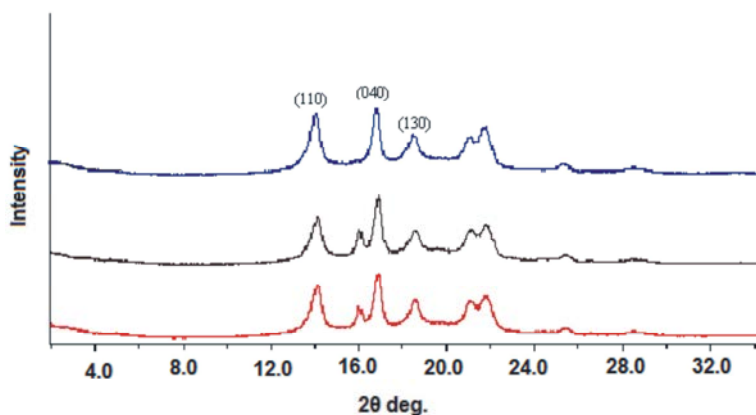


Fig. 2: XRD patterns of TPNR-MWCNT composite with (a) 0 phr, (b) 3phr, (c) 5phr,

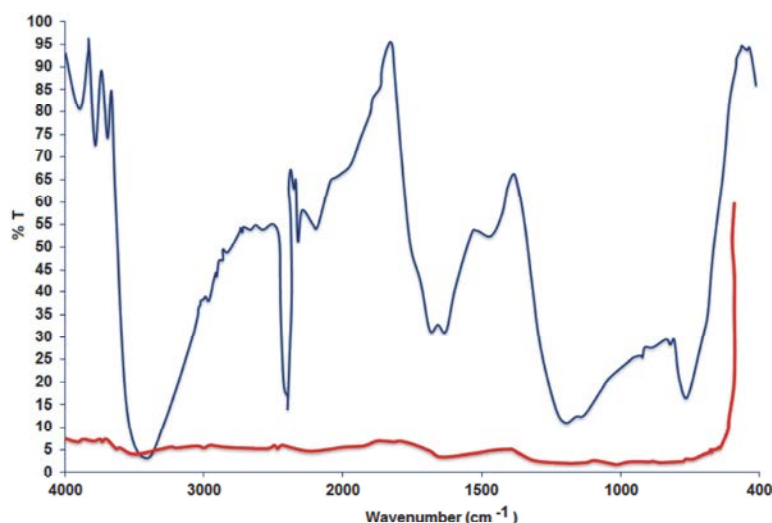


Fig. 3: FTIR spectra of MWCNTs (before acid treatment and after acid treatment)

decrease in the tensile strength. This supports our results for thermal behavior, which due to the kinks or twists of CNTs can affect the thermal conductivity. Figure 4 E. The figure clearly shows a large number of unbroken carbon nanotubes but less than Figure 4 F indicating a poor polymer/nanotube adhesion which is attributed to the reduction in the properties of TPNR/MWCNTs nanocomposites.

### Mechanical Properties

**Tensile Strength:** The tensile strengths of TPNR reinforced with MWCNTs (with and without treatment) of different percentages (1%, 3%, 5% and 7%) are shown in Figure 5. Generally, both MWCNTs exhibited an increasing trend up to 3wt% content. Further increments in MWCNTs content decreased the tensile strength compared to the optimum filler loading. From Figure 5, TPNR with UTMWCNTs and TMWCNTs have optimum results at 3 wt%, which, compared with TPNR, increased by 23% and 39%, respectively. The improvement in the tensile strength may be caused by the good dispersion of MWCNTs in the TPNR matrix, which leads to a strong interaction between the TPNR matrix and MWCNTs. The order of these value is TPNR/TMWCNTs > TPNR/UTMWCNTs > TPNR. The better properties in tensile strength for the TPNR/TMWCNTs nanocomposites could be due to the improved dispersion of the MWCNTs, as well as the response to the opportunities offered by the acid treated MWCNTs [27].

**Young's Modulus:** Figure 7 shows the effect of filler content on the tensile modulus of TPNR reinforced by TMWNTs and UTMWCNTs. The same trend as for the

tensile strength in Figure 6 was observed for the tensile modulus of TMWCNTs. Figure 6 clearly shows that the presence of MWCNTs has significantly improved the tensile modulus of the TPNR. The remarkable increase of Young's modulus with TMWCNTs content shows a greater improvement than that seen in the tensile strength at high content, which indicates that the Young's modulus increases with an increase in the amount of the TMWCNTs. At 3 wt% of TMWCNTs the Young's modulus is increased by 34 % compared to TPNR. The Young's modulus of UTMWCNTs increased with the increase in the amount of UTMWCNTs. The maximum result was achieved at 3wt%, with an increase of about 22%, which was due to the good dispersion of nanotubes displaying perfect stress transfer [27]. The improvement of modulus is due to the high modulus of MWCNTs [28]. The further addition of TMWCNTs and UTMWCNTs from 5 to 7 wt% increased the Young modulus dropped respectively.

**Impact Strength:** The effect of filler loading on the impact strength of TPNR/TMWCNTs and TPNR/UTMWCNTs nanocomposites is given in Figure 7. It shows that incorporation of MWCNTs into TPNR considerably affects the impact strength of TPNR nanocomposites. The results exhibited better impact strength for TMWCNTs and UTMWCNTs at 3 wt% with an increase of about 82% and 46%, respectively. This is due to the better dispersion of carbon nanotubes in the matrix, which generated a significant toughening effect on the TPNR/ TMCWNTs nanocomposite compared with TPNR/UTMWCNTs nanocomposites. However, when the load is transferred to the physical network between the

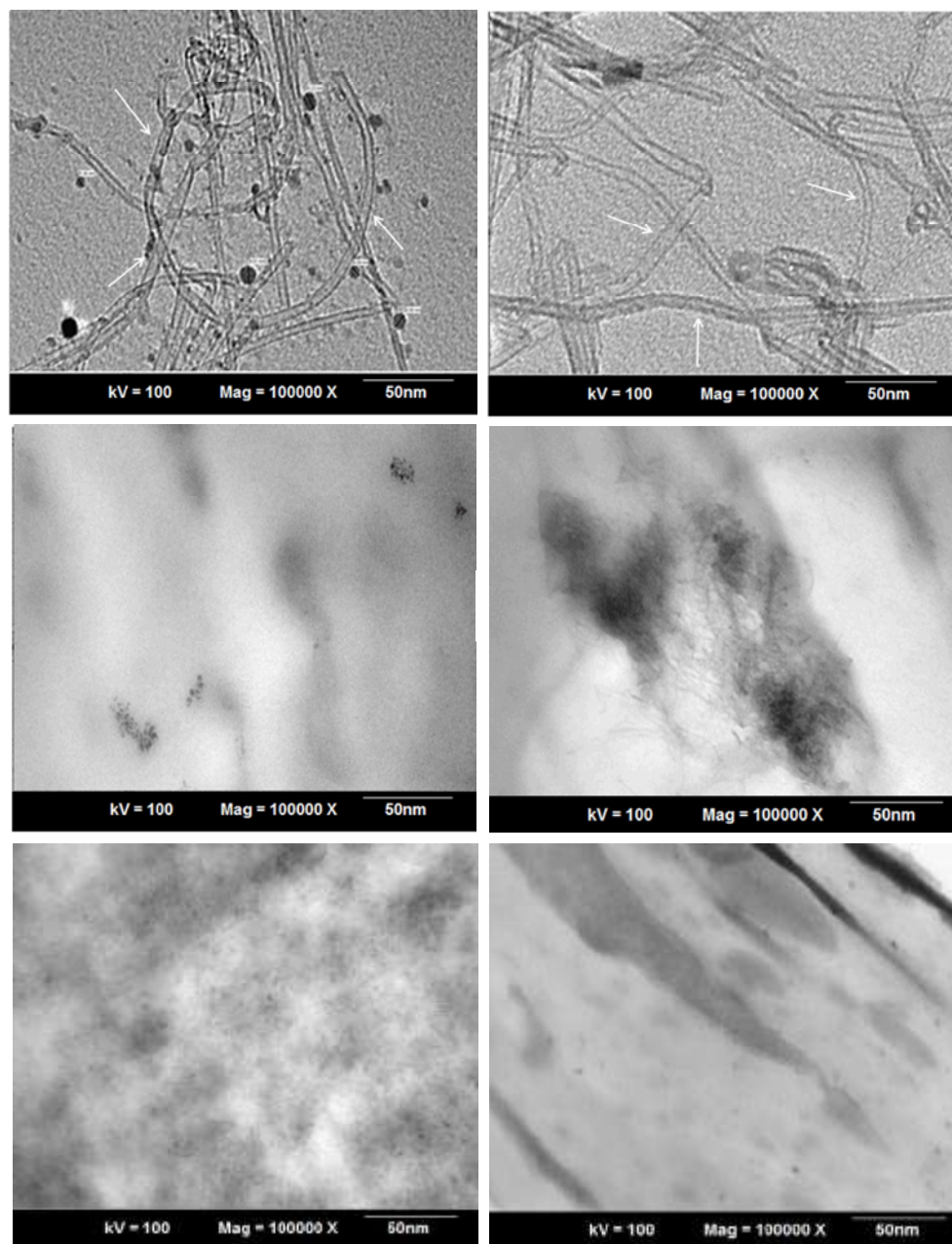


Fig. 4: TEM micrograph of Pure MWCNTs before acid treatment with different magnifications (A)after acid treatment with different magnifications (B)TPNR with 1wt% UTMWCNTs.(C) TPNR with 3wt% UTMWCNTs (D) TPNR with 1wt% TMWCNTs (E) TPNR with 3wt% TMWCNTs (F)

matrix and the filler, the debonding of the chain segments from the filler surface facilitates the relaxation of the matrix entanglement structure, leading to higher impact toughness. The low impact energy was attributed to the filler content being more than 3wt%. This will reduce the ability of reinforced composites to absorb energy during fracture propagation. This will lead to less energy dissipating in

the system due to the poor interfacial bonding and induces micro spaces between the filler and polymer matrix [29].

#### Thermal Properties

**Glass Transition Temperature:** The dynamic mechanical data shows that the glass transition temperature of the TPNR/ UTMWCNTs and TPNR/TMWNTs is affected



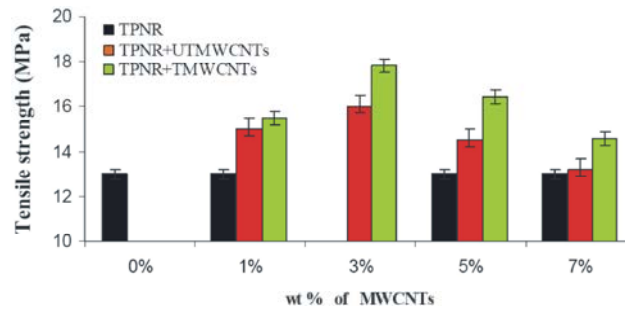


Fig. 5: Tensile strength of TPNR reinforced with MWCNTs (with and without treatment)

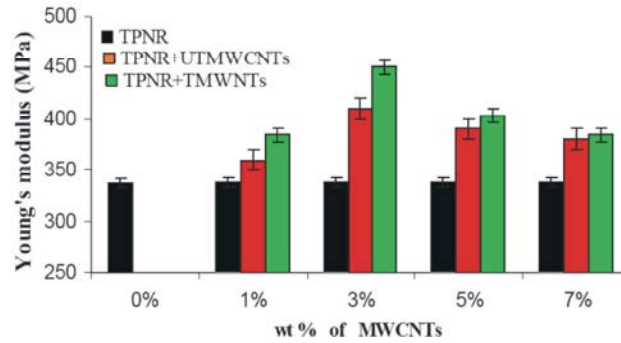


Fig. 6: Young's Modulus of TPNR reinforced with MWCNTs (with and without treatment)

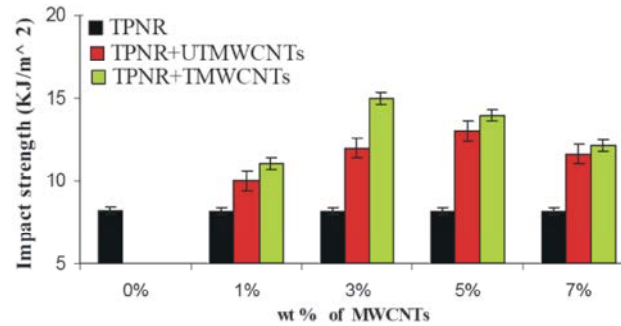


Fig. 7: Impact Strength of TPNR reinforced with MWCNTs (with and without treatment)

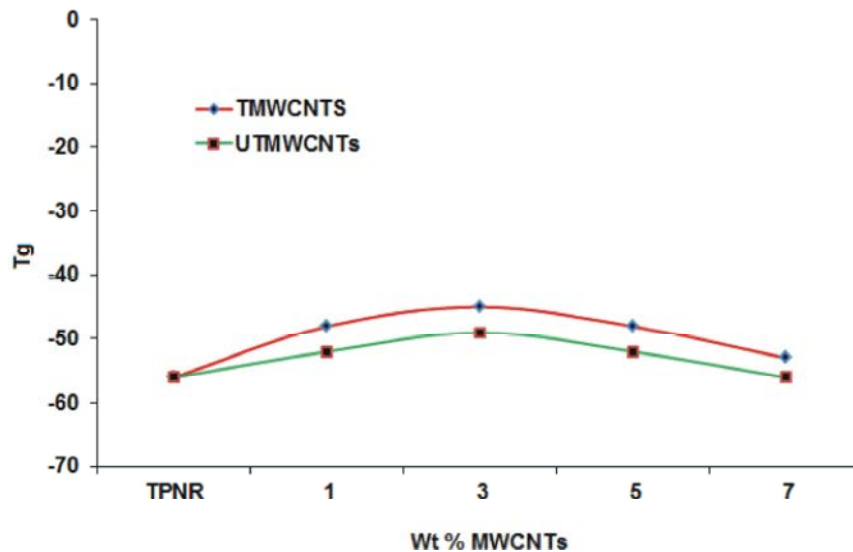


Fig. 8: Glass Transition Temperature of TPNR reinforced with MWCNTs (with and without treatment)

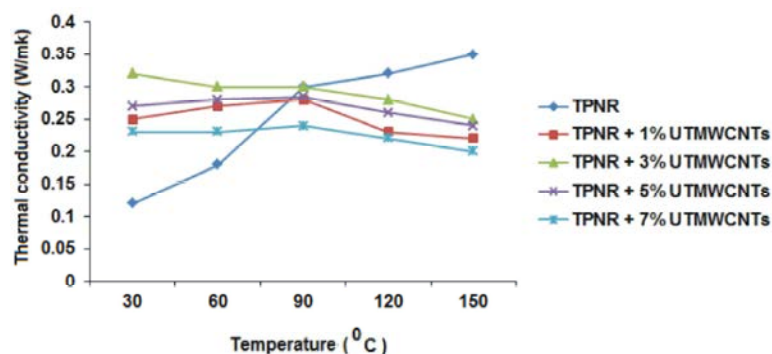


Fig. 9: Thermal Conductivity of TPNR reinforced with UTMWCNTs

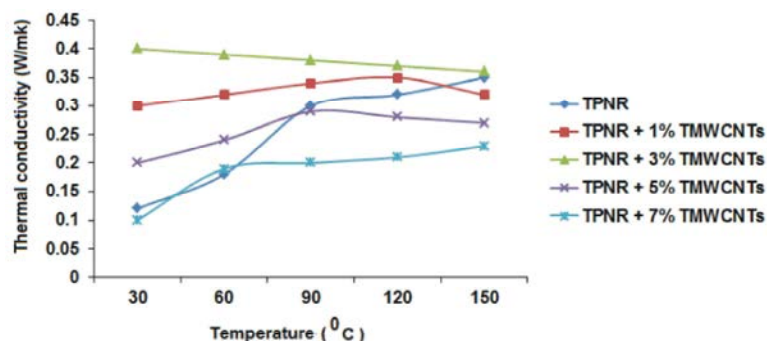


Fig. 10: Thermal Conductivity of TPNR reinforced with TMWCNTs

by the addition of the different amounts of MWCNTs, as depicted in Figure 8. From the figures, the  $T_g$  for the TPNR/TMWCNTs nanocomposites is higher than the corresponding temperature for the TPNR and TPNR/UTMWCNTs nanocomposites, usually the  $T_g$  of a polymeric matrix tends to increase with the addition of carbon nanotubes. The rise in  $T_g$  in any polymeric system is associated with a restriction in molecular motion, reduction in free volume and/or a higher degree of crosslinking (TPNR/TMWCNTs > TPNR/UTMWCNTs) due to the interactions between the polymer chains and the nanoparticles and the reduction of macromolecular chain mobility. With the high amount of MWCNTs (after 3wt %) of TMWCNTs and UTMWCNTs the  $T_g$  drops. This might be due to the phase separation/agglomeration of MWCNTs, this allows the macromolecules to move easily.

**Thermal Conductivity:** To study the effect of MWCNTs filler on thermal conductivity, the temperature was varied from (30-150)°C. The carbon filler loading was from 1wt% to 7wt% for two types of carbon nanotubes (UTMWCNTs and TMWCNTs). Introducing MWCNTs to TPNR can significantly enhance the thermal conductivity of the TPNR matrix, as shown in Figure 9 and Figure 10. As shown in Figure 9 at 30°C the thermal

conductivity of TPNR/TMWCNTs composites, Thermal conductivity increased at 3wt% compared to 1wt%, 5wt% and 7wt%, respectively and for TPNR/UTMWCNTs, the thermal conductivity increased at 3wt%, as compared to TPNR at the same temperature as shown in Figure 12. Thermal transport in the CNT composites includes phonon diffusion in the matrix and ballistic transportation in the filler. As shown in Figure 9 and Figure 10, the thermal conductivity of TMWCNTs reinforced TPNR matrix composites for all volume fractions studied from 30°C to 150°C is better than UTMWCNTs. The effect of temperature on the thermal conductivity is clear from 30°C to 90°C, as shown in the figures. This is because of the opposing effect of temperature on the specific heat and thermal diffusivity. Eventually, at high temperatures, as the phonon mean free path is lowered, the thermal conductivity of the matrix approaches the lowest limit and the corresponding thermal resistivity approaches the highest limit [30].

## CONCLUSION

TPNR nanocomposites were prepared by melt blending of PP, NR and LNR with MWCNTs were successfully synthesized via in situ polymerization method. The TEM micrograph has shown that the effect

of acid treatment has roughened the MWCNTs surface and also reduced the agglomeration. Various functional groups have been confirmed using FTIR. The TPNR nanocomposite was prepared using the melt blending method. MWCNTs are incorporated in the TPNR nanocomposite at different compositions which is 1, 3, 5 and 7 wt%. The addition of MWCNTs in the TPNR matrix improved the mechanical properties. At 3wt%, the tensile strength and Young's modulus of TPNR/UTMWCNTs increased 23% and 22%, respectively. For TPNR/TMWCNTs the optimum result of tensile strength and Young's modulus was recorded at 3% which increased 39% and 34%, respectively. In the addition the elongation of break decreased by increasing the amount of both types of MWCNTs.

#### ACKNOWLEDGEMENTS

The authors would like to thank the CIPET Bhubaneswar, India for characterization.

#### REFERENCES

1. Liu, X., M. Wang, S. Zhang and B. Pan, 2013. Application potential of carbon nanotubes in water treatment: A review. *J. Environ. Sci. (China)*, 1; 25(7): 1263-80. PMID: 24218837.
2. Wong, B.S., S.L. Yoong, A. Jagusiak, T. Panczyk, H.K. Ho, W.H. Ang and G. Pastorin, 2013. Carbon nanotubes for delivery of small molecule drugs. *Adv Drug Deliv Rev.* doi:p11: S0169-409X(13)00188-9. 10.1016/j.addr.2013.08.005. PMID: 23954402.
3. Lu, W., M. Zu, J.H. Byun, B.S. Kim and T.W. Chou, 2012. State of the art of carbon nanotube fibers: opportunities and challenges. 2012 *Adv Mater.*, 24(14): 1805-33. doi: 10.1002/adma.201104672. PMID: 22438092.
4. Arsecularatne, J.A. and L.C. Zhang, 2007. Carbon nanotube reinforced ceramic composites and their performance. *Recent Pat Nanotechnol.*, 1(3): 176-85. PMID: 19076031.
5. Miyagawa, H., M. Misra and A.K. Mohanty, 2005. Mechanical properties of carbon nanotubes and their polymer nanocomposites. *J. Nanosci. Nanotechnol.*, 5(10): 1593-615. PMID: 16245518.
6. Lin, Y., W. Yantasee and J. Wang, 2005. Carbon nanotubes (CNTs) for the development of electrochemical biosensors. *Front Biosci*, 1(10): 492-505. Print 2005 Jan 1. PMID: 15574386.
7. Roy, S., T. Das, C.Y. Yue and X. Hu, 2013. Improved Polymer Encapsulation on Multiwalled Carbon Nanotubes by Selective Plasma Induced Controlled Polymer Grafting. *ACS Appl Mater Interfaces*. 19 PMID: 24191852.
8. Mahmoodian, H., O. Moradi and B. Shariatzadeh, 2013. Grafting chitosan and polyHEMA on carbon nanotubes surfaces: "Grafting to" and "Grafting from" methods. *Int J. Biol. Macromol.*, 29; 63C: 92-97. doi: 10.1016/j.ijbiomac.2013.10.030. PMID: 24183808.
9. Sen, F., A.A. Boghossian, S. Sen, Z.W. Ulissi, J. Zhang and M.S. Strano, 2012. Observation of oscillatory surface reactions of riboflavin, trolox and singlet oxygen using single carbon nanotube fluorescence spectroscopy. *ACS Nano*. Dec., 21; 6(12): 10632-45. doi: 10.1021/nn303716n. Epub 2012 Dec 7. PMID: 23075271
10. Zhao, L., Y. Li, X. Cao, J. You and W. Dong, 2012. Multifunctional role of an ionic liquid in melt-blended poly (methyl methacrylate)/ multi-walled carbon nanotube nanocomposites. *Nanotechnology*, 23(25): 255702. doi: 10.1088/0957-4484/23/25/255702. Epub 2012 May 31. PMID: 22652559.
11. Liao, C.Z., K. Li, H.M. Wong, W.Y. Tong, K.W. Yeung and S.C. Tjong, 2013. Novel polypropylene/biocomposites reinforced with carbon nanotubes and hydroxyapatite nanorods for bone replacements. *Mater Sci. Eng. C Mater Biol. Appl.*, 33(3): 1380-8. doi: 10.1016/j.msec.2012.12.039. Epub 2012 Dec 13. PMID: 23827585.
12. Shim, Y.S. and S.J. Park, 2012. Rheological and mechanical properties of polypropylene prepared with multi-walled carbon nanotube masterbatch. *J. Nanosci Nanotechnol.*, 12(7): 5972-5. PMID: 22966691.
13. Song, P., Y. Shen, B. Du, Z. Guo and Z. Fang, 2009. Fabrication of fullerene-decorated carbon nanotubes and their application in flame-retarding polypropylene. *Nanoscale*. Oct; 1(1): 118-21. doi: 10.1039/b9nr00026g. Epub 2009 Aug 28. PMID: 20644869.
14. Du, B. and Z. Fang, 2010. The preparation of layered double hydroxide wrapped carbon nanotubes and their application as a flame retardant for polypropylene. *Nanotechnology*. Aug 6; 21(31): 315603. doi: 10.1088/0957-4484/21/31/315603. Epub 2010 Jul 15. PMID: 20634567
15. Sae-Khow, O. and Mitra S. Simultaneous, 2010. Extraction and concentration in carbon nanotube immobilized hollow fiber membranes. *Anal Chem*. Jul 1; 82(13): 5561-7. doi: 10.1021/ac100426y. PMID: 20518469.



16. Gao, Y., M. Shi, R. Zhou, C. Xue, M. Wang and H. Chen, 2009. Solvent-dependent fluorescence property of multi-walled carbon nanotubes noncovalently functionalized by pyrene-derivatized polymer. *Nanotechnology*, 20(13): 135705. doi: 10.1088/0957-4484/20/13/135705. Epub. PMID: 19420514.
17. Xue, C.H., M.M. Shi, Q.X. Yan, Z. Shao, Y. Gao, G. Wu, X.B. Zhang, Y. Yang, H.Z. Chen and M. Wang, 2008. Preparation of water-soluble multi-walled carbon nanotubes by polymer dispersant assisted exfoliation. *Nanotechnology*. Mar 19; 19(11): 115605. doi: 10.1088/0957-4484/19/11/115605. Epub PMID: 21730556.
18. Maggini, L., F. De Leo, R. Marega H.M. Tóhátí, K. Kamarás and D. Bonifazi, 2011. Carbon nanotube-based metal-ion catchers as supramolecular depolluting materials. *Chem. Sus. Chem.*, Oct 17; 4(10): 1464-9. doi: 10.1002/cssc.201100163. Epub. PMID: 21905238.
19. Chen, Z., D. Pierre, H. He, S. Tan, C. Pham-Huy, H. Hong and J. Huang, 2010. Adsorption behavior of epirubicin hydrochloride on carboxylated carbon nanotubes. *Int J. Pharm.*, 405(1-2): 153-61. doi: 10.1016/j.ijpharm.11.034. Epub. PMID: 21145959.
20. Ji, L., W. Chen, J. Bi, S. Zheng, Z. Xu, D. Zhu and P.J. Alvarez, 2010. Adsorption of tetracycline on single-walled and multi-walled carbon nanotubes as affected by aqueous solution chemistry. *Environ Toxicol Chem.* 2010 Dec; 29(12): 2713-9. doi: 10.1002/etc.350. Epub. PMID: 20836069.
21. Anik, U., S. Cevik and M. Pumera, 2010. Effect of Nitric Acid "Washing" Procedure on Electrochemical Behavior of Carbon Nanotubes and Glassy Carbon  $\mu$ -Particles. *Nanoscale Res. Lett.*, 16; 5(5): 846-52. doi: 10.1007/s11671-010-9573-6. PMID: 20672081.
22. Salavati-Niasari, M., F. Davar and M. Bazarganipour, 2010. Synthesis, characterization and catalytic oxidation of para-xylene by a manganese(III) Schiff base complex on functionalized multi-wall carbon nanotubes (MWNTs). *Dalton Trans.*, 39(31): 7330-7. doi: 10.1039/b923416k. Epub 2010 Jul 2. PMID: 20601980.
23. Neelgund, G.M. and A. Oki, 2011. Nanoparticles deposited on poly(lactic acid) grafted carbon nanotubes: synthesis, characterization and application in Heck C-C coupling reaction. *Appl Catal A Gen.*, 399(1-2): 154-160. PMID: 21731192.
24. Seung, H.L., C. Eunnari, H.J. So and R.Y. Jae, 2007. Rheological and electrical properties of polypropylene composites containing functionalized multi-walled carbon nanotubes and compatibilizers. *Carbon*, 45: 2810-2822.
25. Hirsch, A., 2002. Functionalization of single-walled carbon nanotubes. *Angew. Chem. Int. Ed*, 41: 1853-1859.
26. Vishnu, N., A.S. Kumar and K.C. Pillai, 2007. Unusual neutral pH assisted electrochemical polymerization of aniline on a MWCNT modified electrode and its enhanced electro-analytical features. *Analyst*, 138(21): 6296-300. doi: 10.1039/c3an01067h. PMID: 23998181.
27. Kim, H.S., S.M. Kwon, K.H. Lee, J.S. Yoon and H.J. Jin, 2008. Preparation and characterization of silicone rubber/functionalized carbon nanotubes composites via in situ polymerization. *J Nanosci. Nanotechnol.* Oct; 8(10): 5551-4. PMID: 19198496.
28. Sepúlveda, A.T., R. Guzman De Villoria, J.C. Viana, A.J. Pontes, B.L. Wardle and L.A. Rocha, 2013. Full elastic constitutive relation of non-isotropic aligned-CNT/PDMS flexible nanocomposites. *Nanoscale*. 2013 Jun 7; 5(11): 4847-54. doi: 10.1039/c3nr00753g. Epub. PMID: 23616092.
29. Badrinarayanan, P., J. Leonard and M.R. Kessler, 2011. Enhanced reaction kinetics and impact strength of cyanate ester reinforced with multiwalled carbon nanotubes. *J Nanosci. Nanotechnol.*, 11(5): 3970-8. PMID: 21780394.
30. Li, W., Y. Zhang, J. Yang, J. Zhang, Y. Niu and Z. Wang, 2012. Thermal annealing induced enhancements of electrical conductivities and mechanism for multiwalled carbon nanotubes filled poly(ethylene-co-hexene) composites. *ACS Appl Mater Interfaces.*, 4(12): 6468-78. doi: 10.1021/am302597f. Epub 2012 Dec 4. PMID: 23173546.